High-Pressure Near-Infrared Raman Spectroscopy of Bacteriorhodopsin Light to Dark Adaptation

Alfons Schulte and Larry Bradley II
Department of Physics and Center for Research and Education in Optics and Lasers University of Central Florida, Orlando, Florida 32816-2385 USA

ABSTRACT Near-infrared (NIR) Raman spectroscopy is employed as an in situ probe of the chromophore conformation to study the light to dark-adaptation process in bacteriorhodopsin (bR) at variable pressure and temperature in the absence of undesired photoreactions. In dark-adapted bR deconvolution of the ethylenic mode into bands assigned to the all-*trans* (1526 cm^{-1}) and 13-*cis* (1534 cm^{-1}) isomers yields a 13-*cis* to all-*trans* ratio equal to 1 at ambient pressure (Schulte et al., 1995, *Appl. Spectrosc.* 49:80–83). Detailed spectroscopic evidence is presented that at high pressure the equilibrium is shifted toward the 13-*cis* isomers and that the light to dark adaptation kinetics is accelerated. The change in isomeric composition with temperature and pressure as well as the kinetics support a two-state model with activation volumes of −16 ml/mol for the transition of 13-*cis* to all-*trans* and −22 ml/mol for the reverse process. These compare with a conformational volume difference of 6.6 ml/mol, which may be attributed to the ionization of one or two residues or the formation of three hydrogen bonds.

INTRODUCTION

Bacteriorhodopsin (bR) is a retinal protein found in the purple membrane of the bacterium *Halobacterium halobium* that functions as a light-driven proton pump. By absorbing photons of visible light, bacteriorhodopsin transports protons across the cell membrane. The resulting transmembrane proton gradient provides electrochemical energy that is used by the cell in many ways, including the synthesis of ATP (Oesterhelt and Stoecknius, 1971; Birge, 1990; Lanyi, 1992). A three-dimensional electron density map with a resolution of several angstroms has been constructed from electron diffraction experiments (Henderson et al., 1990). The proton transport from the inside of the cell to the extracellular medium is connected to a photochemical reaction photocycle with several intermediates that have been characterized by the absorption and resonance Raman spectra of the chromophore (Mathies et al., 1991). Resonance Raman spectroscopy in particular has been crucial to the interpretation of the chromophore structure during the photocycle (Stockburger et al., 1986; Mathies et al., 1987). The general features of the proton transport and the kinetics of the chromophore during the photocycle are understood, and they require that the protein undergo crucial conformational transitions (Henderson et al., 1990; Mathies et al., 1991).

In the resting state bR exists in two distinct forms, light-adapted and dark-adapted. Light-adapted bR is the starting conformation for the photocycle, and the chromophore is in an all-*trans* configuration. If left in the dark for prolonged periods of time, light-adapted bR (bR^{LA}) slowly transforms into another form, called dark-adapted bacteriorhodopsin (bR^{DA}). bR^{DA} is a mixture of all-*trans* and 13-*cis* pigments, and from chromatographic analysis an isomeric ratio close to 1 has generally been found (Oesterhelt et al., 1973; Pettei et al., 1977; Dencher et al., 1983; Tsuda and Ebrey, 1980), although there has been some debate as to the ratio of all-*trans* to 13-*cis* isomers in bR^{DA} at atmospheric pressure (Scherrer et al., 1989).

The rapid development of near-infrared (NIR) Raman spectroscopy has opened a new approach to studying the molecular structure of photosensitive compounds (Mattioli et al., 1993). By shifting the excitation wavelength into the near-infrared Raman spectra can be measured in the absence of photoalteration and fluorescence. This is a distinct advantage over conventional Raman measurements using visible excitation, where rapid flow techniques have been employed to alleviate the inherent problem of light adaptation due to the probe beam and to measure the resonance Raman spectrum of bR^{DA}. Because of the presence of both isomers the determination of the resonance Raman spectrum of the 13-*cis* component from that of bR^{DA} involves a subtraction procedure, which is based on chemical extraction results (Aton et al., 1979; Stockburger et al., 1979). More importantly, near-infrared excitation makes Raman measurement on photolabile proteins in a high-pressure cell feasible, and the preresonance effect can preserve the selective enhancement of chromophore modes. This has provided a spectroscopic approach to determining the composition of retinal isomers in bR in situ (Schulte et al., 1995), yielding a 13-*cis* to all-*trans* ratio in bR^{DA} equal to 1 at atmospheric pressure.

As a thermodynamic parameter pressure is as important as temperature for the energetics of a chemical reaction. The study of high-pressure effects is of considerable interest, because the intermolecular interactions can be altered without major perturbations caused by variations in temperature or chemical composition. Thus thermal and volume effects

Received for publication 17 April 1995 and in final form 5 July 1995.
Address reprint requests to Dr. Alfons Schulte, Department of Physics, University of Central Florida, Orlando, FL 32816-2385. Tel.: 407-823-5196; Fax: 407-823-5112; E-mail: AFS@PHYS.PHYSICS.UCF.EDU.

0006-3495/95/10/1554/09 $2.00

can be separated. Pressure below 200 MPa can induce conformational changes in proteins (Weber and Drickamer, 1983; Jonas and Jonas, 1994) and affect the kinetics of a chemical reaction as well. Depending on the sign of the activation volume the rate can either increase or decrease (Frauenfelder et al., 1990). High-pressure experiments on bR have essentially been limited to a few absorption studies. Tsuda and Ebrey (1980) relied on chemical extraction methods to explain spectral changes of the visible absorption bands in bR^{DA} at high pressure with a change in the equilibrium constant favoring $bR^{13\text{-}cis}$. Other absorption experiments have shown that pressure alters the kinetics of the photocycle (Marque and Eisenstein, 1984) and dark adaptation (Kovacs et al., 1993). Unfortunately, the rather featureless absorption bands prohibit a direct determination of the chromophore structure. This problem can be overcome by Raman spectroscopy. However, with the exception of a brief report that structurally identifies an increase of the 13-*cis* component at high pressure (Schulte et al., 1995), data are absent. This may perhaps be attributed to experimental difficulties, which are removed now because of recent progress in laser excitation sources and detection systems with sensitivity near the single photon level in the near-infrared.

In this paper we present the first high-pressure study of bR light to dark adaptation kinetics employing NIR Raman spectroscopy as an in situ probe for the chromophore structure. Deconvolution of the ethylenic mode shows that both the equilibrium ratio of 13-*cis* to all-*trans* isomers and the rate of dark adaptation increase with increasing pressure. The temperature dependence of the kinetics yields the activation energies. The molar volumes for the $bR^{all\text{-}trans}$ to $bR^{13\text{-}cis}$ conversion are determined from the pressure dependence and discussed in terms of conformational changes.

MATERIALS AND METHODS

Near-infrared excitation (840 nm) was obtained from a Ti:sapphire laser (Schwartz Electro-Optics, Orlando, FL) which was pumped by a 6-W Ar ion laser (model 306, Coherent, Palo Alto, CA). Raman scattered light is dispersed with a single-grating spectrograph (HR640, Instruments SA, Edison, NJ) and detected with a charge-coupled device detector (LN/CCD-1024TKB, Princeton Instruments, Trenton, NJ). A semiconductor bandgap filter (II–VI Inc., Saxonburg, PA) provides efficient rejection of the Rayleigh line. Individual spectra were acquired in less than 100 with 50–100 mW of laser power. A schematic of the experimental setup is shown in Fig. 1.

For high-pressure measurements the bR sample was sandwiched between two sapphire windows using a doughnut-shaped spacer of 1 mm thickness and ≈3 mm hole diameter. This assembly was contained in a high-pressure cell made from beryllium-copper, using nitrogen gas as the pressure-transmitting medium. Optical access was provided by two axial sapphire windows with an f-number of 1.9. High pressure was generated with an air-driven compressor (model 46–14060–2, Newport Scientific, Jessup, MD) and measured with a Bourdon gauge accurate to 4 MPa. The high-temperature cell attaches to the head of a refrigerator, allowing measurements in the range of 10–350 K. Temperatures above 294 K were maintained with a heater wire and a temperature controller (DRC 93CA, Lakeshore, Westerville, OH). A silicon diode sensor mounted on the high-pressure cell monitored the temperature, which was stable to 0.1 K.

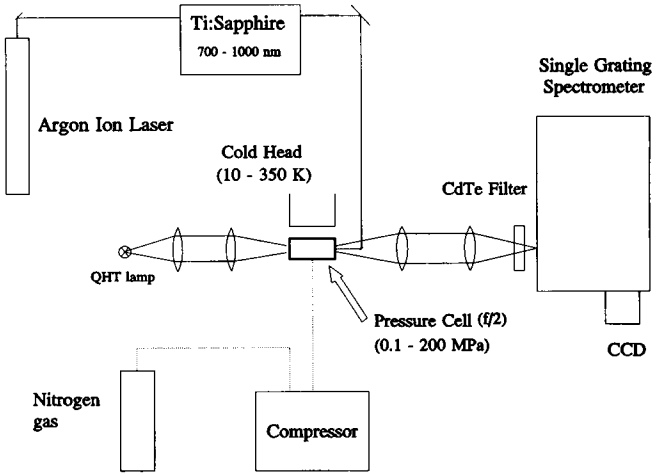

FIGURE 1 Schematic of the experimental setup for high-pressure Raman spectroscopy.

Purple membranes were in aqueous solution at a pH near 7. No buffer was added because of potential complications of the effect of pressure on the pH of the buffer. The optical density of the samples was between 2 and 6 at 568 nm at an optical pathlength of 1 mm. The bacteriorhodopsin samples were dark-adapted by 20-h incubation at 300 K. Light adaptation was achieved by 10-min illumination with a 250-W quartz halogen tungsten lamp (model 66184, Oriel, Stratford, CT) equipped with heat and yellow glass filters. Once light adaptation is completed, the sample is left at constant pressure and constant temperature for the entire experiment. The spectra for the light-adapted state were measured immediately after the light source was shut off. To monitor the dark adaptation, Raman spectra were taken at subsequent times under identical conditions.

RESULTS AND DISCUSSION

Near-infrared Raman spectroscopy at ambient pressure

The Raman spectra of bacteriorhodopsin during light to dark adaptation excited in the near-infrared are depicted in Fig. 2. The spectrum of bR^{LA} ($t = 0$) is dominated by vibrational bands of the all-*trans*-retinal Schiff base chromophore (Mathies et al., 1987). Spectra taken at subsequent times while the sample was left in complete darkness show the addition of a peak at 1536 cm^{-1}, corresponding to the 13-*cis* isomer. Similarly, there are consistent changes in the fingerprint region. As expected, this indicates that the sample is slowly changing from light-adapted bR to dark-adapted bR in the absence of light. The similarity of the spectrum obtained in the near-infrared with those recorded in the visible indicates a preresonance condition for 841 nm excitation. This finding is in agreement with other recent NIR Raman studies (Johnson and Rubinovitz, 1991; Sawatzki et al., 1990; Schulte, 1992; Rath et al., 1993), and it has been attributed to preresonance enhancement of the vibronic contribution (Albrecht's B-term) (Sawatzki et al., 1990; Johnson and Rubinovitz, 1991). However, in some of the FT-Raman spectra complete light adaptation could not be obtained because of the high concentration of the sam-

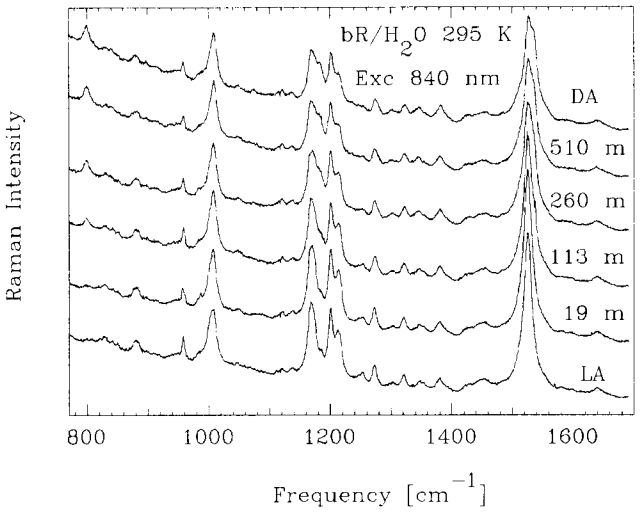

FIGURE 2 NIR Raman spectra of the light to dark adaptation kinetics at atmospheric pressure (T = 295 K). The times after completion of light adaptation are given in minutes. Raman scattering was excited with 50 mW of 840 nm light. Individual spectra were acquired in 100 s with a spectral resolution of 3 cm^{-1}. The spectra were not corrected for the instrument profile, nor was any smoothing or background subtraction performed.

ples requiring corrections, such as subtracting the spectrum of a fully dark-adapted sample (Rath et al., 1993). Fig. 2 also demonstrates that our samples were fully light-adapted and that they exhibit native Raman spectra with near-infrared excitation. It appears that the approach of combining a single grating spectrograph and a back-illuminated CCD detector results in a higher sensitivity based on a comparison of integration time, spectral resolution, and sample concentration as compared to published FT Raman spectra. Thus we present the raw data without corrections or smoothing. The vibrational analysis of the resonance Raman spectra of bR^{LA} and bR^{DA} has been discussed in detail by Mathies and co-workers (Smith et al., 1987a,b) The most intense bands are due to the ethylenic C=C stretching modes. We observe maxima at 1526 cm^{-1} and 1534 cm^{-1} for the all-*trans* and the 13-*cis* isomers, respectively. The NIR Raman spectra clearly demonstrate that the chromophore in the light-adapted sample is in the all-*trans* configuration, whereas the spectrum of bR^{DA} shows a mixture of all-*trans* and 13-*cis*. This is evident from the double-peaked structure of the ethylenic mode with maxima at 1526 and 1534 cm^{-1}, as well as from the bands in the fingerprint region between 1160 and 1250 cm^{-1}, which are highly sensitive to isomerization. The peak at 1639 cm^{-1} corresponds to the Schiff base linkage (C=NH) of the chromophore to the protein. The band at 800 cm^{-1} is only present in bR^{DA} and it has been assigned to the $C_{14}H$ hydrogen out-of-plane (HOOP) mode (Smith, 1987b). Successive measurements on the dark-adapted sample did not show a change in the spectrum, indicating the absence of photoconversion due to the NIR laser beam. The advantage of using excitation near 840 nm is that we can probe the dark-adapted form of bacteriorhodopsin without initiating photoconversion, and the preresonance effect allows us to preserve the selectivity of observing chromophore modes. This approach lends itself to high-pressure studies.

Identification of chromophore structure during dark adaptation at high pressure

Pressure can affect proteins in two distinct ways (Frauenfelder et al., 1990). First, it can alter the equilibrium population between different conformational states. Second, it also changes the reaction rate coefficient. To start with, we give a detailed account of the pressure and temperature dependence of the isomeric ratio obtained directly from the Raman spectra, and pressure effects on the kinetics of dark adaptation are discussed in the next section.

Pressure and temperature dependence of the 13-*cis* to all-*trans* equilibrium

The pressure dependence of the NIR Raman spectrum of bR^{DA} in the ethylenic region is shown in Fig 3. In these experiments the sample was first allowed to completely dark adapt at atmospheric pressure (0.1 MPa) and constant temperature. Raman spectra were then taken at various pressures, ranging from 0.1 MPa to 170 MPa, after waiting several hours to allow the sample to arrive at a new equilibrium at each hydrostatic pressure. In contrast to the visible absorption bands, which are rather featureless, the Raman spectra exhibit distinct structure, such as the ethylenic modes with maxima at 1526 and 1536 cm^{-1}. We observe that the peak at 1536 cm^{-1} corresponding to the 13-*cis* isomer increases in intensity with increased pressure. This confirms a previous brief report, where experiments were restricted to pressures of 0.1 and 165 MPa (Schulte et al., 1995). If the probe beam would initiate a photoconversion toward the light-adapted state, the opposite effect would occur. Similarly, the fingerprint region shows an increase of the C-C single bond stretches of 13-*cis* (Fig. 6). Hence, high pressure shifts the isomeric equilibrium in dark-adapted bR toward the 13-*cis* isomer.

The isomeric ratio is determined by following the procedure described previously (Schulte et al., 1995). For the Raman scattered intensity, we can assume that the area of the peak is proportional to the product of the scattering cross section and the population of the particular conformation (Long, 1977; Mathies et al., 1987), specifically the all-*trans* or 13-*cis* isomers. In NIR Raman experiments of bR^{LA} we observe no detectable difference between the spectra taken at atmospheric pressure and at 170 MPa. The peak intensities are identical, and frequency shifts are less than 2 cm^{-1}. This implies that the Raman scattering cross sections are pressure independent. Our analysis of dark-adapted bR has revealed that the ratio of the scattering cross sections $\sigma_{\text{all-}trans}$ to $\sigma_{13\text{-}cis}$ is 4 (Schulte et al., 1995). This is to be expected because of the slightly different positions of the absorption maxima and different extinction coefficients for

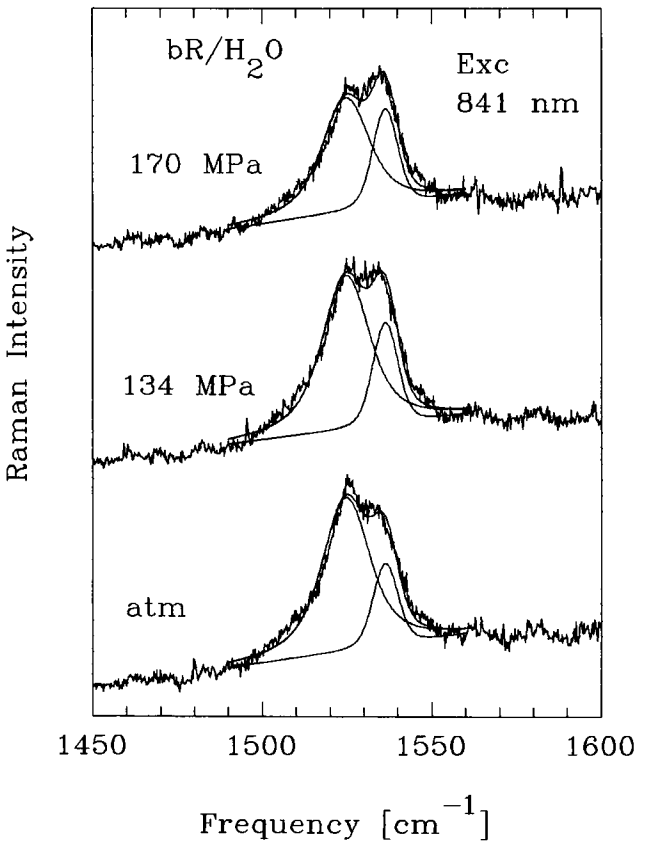

FIGURE 3 Effect of high pressure on the Raman spectrum of dark-adapted bacteriorhodopsin in the region of the ethylenic mode. The spectra have been shifted by a constant along the vertical axis for clarity. The entrance slit of the spectrograph was set to give a resolution of 2 cm^{-1} at an excitation wavelength of 840 nm. The accumulation time for each spectrum was 100 s at a laser power of 50 mW. Deconvolution using Voigtian line profiles is shown by dashed lines. Note the increase of the 13-*cis* component with increasing pressure. The 13-*cis* to all-*trans* ratios are 0.95, 1.15, and 1.5 for pressures of 0.1, 134, and 170 MPa, respectively.

the 13-*cis* and all-*trans* isomers. However, in the method employed the Raman scattering cross sections cancel, because the total number of molecules is constant and the isomeric ratio K_I can be expressed via the areas of all-*trans* bands only (Schulte et al., 1995):

$$K_I = \frac{A_{\text{all-}trans}(0)}{A_{\text{all-}trans}(\infty)} - 1. \quad (1)$$

$A_{\text{all-}trans}$ (0) and $A_{\text{all-}trans}$ (∞) denote the areas of the respective peaks in light-(t = 0) and dark-adapted bR (t = ∞).

The isomeric ratio determined by deconvolution of the ethylenic mode with Voigtian line profiles is shown as a function of pressure in Fig. 4. From repeated experiments we find the isomeric ratio at atmospheric pressure from this method to be K_I = 1 with an error estimate of 10% (Schulte et al., 1995). This value agrees with results from most of the extraction experiments (Oesterhelt et al., 1973; Pettei et al., 1977; Dencher et al., 1983; Tsuda and Ebrey, 1980). The advantage of the new approach is that the ratio of 13-*cis* to all-*trans* isomers is determined spectroscopically in situ. The major contributions to the experimental errors are small fluctuations in laser power, possible changes in beam alignment, and errors in the areas from the peak-fitting process to the raw spectra.

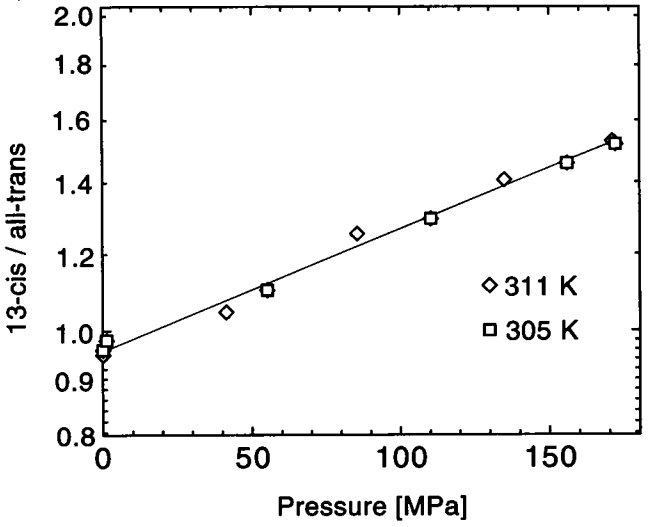

FIGURE 4 Equilibrium ratio of 13-*cis* to all-*trans* isomers in dark-adapted bacteriorhodopsin as a function of pressure at temperatures of 305 and 311 K, respectively.

The effect of temperature on the isomeric ratio in dark-adapted bR at constant pressure is displayed in Fig. 5. Again, the sample was first allowed to completely dark adapt at atmospheric pressure and 295 K. The sample was then raised to various temperatures, ranging up to 310 K, and Raman spectra were recorded. Once the temperature stabilized, the sample was left for 1 h to allow the sample to relax to the new equilibrium. These measurements were repeated to determine the effect of temperature on the isomeric ratio when at hydrostatic high pressure (170 MPa).

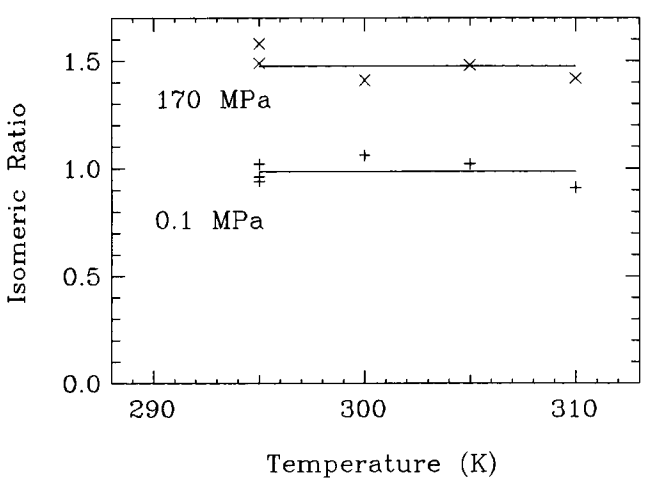

FIGURE 5 Equilibrium ratio of 13-*cis* to all-*trans* isomers in dark-adapted bacteriorhodopsin as a function of temperature at ambient and high pressure (170 MPa).

From this (Fig. 5), we observe that the equilibrium between the all-*trans* and 13-*cis* isomers is independent of temperature at both atmospheric and hydrostatic high pressure.

The equilibrium and kinetic properties of a chemical reaction are determined by the free energy changes. In a simplified picture of a protein with two conformational states the equilibrium ratio between the two states at temperature T and pressure P can be written as (Frauenfelder et al., 1990)

$$K_I(T, P) = \exp\left[-\frac{\Delta G_c(T, P)}{RT}\right] = K_I(T, P_o)\exp\left[-\frac{P\Delta V_c}{RT}\right], \quad (2)$$

where $\Delta G_c(T, P)$ is the conformational free energy difference and R is the universal gas constant.

ΔV_c can be found by monitoring the equilibrium constant (Jonas and Jonas, 1994; Frauenfelder et al., 1990) (here: the isomeric ratio) K_I as a function of pressure. The conformational volume change is given by

$$\Delta V_c = \left.\frac{\partial \Delta G_c(T, P)}{\partial P}\right|_T = -\left.\frac{RT\partial \ln K_I(T, P)}{\partial P}\right|_T. \quad (3)$$

Fig. 4 shows that plots of the logarithm of $1/K_I$ versus pressure at both 305 K and 311 K are linear within experimental error. The conformational volume ΔV_c is determined from the slope of these lines. A least-squares regression on the data for both temperatures yields values for the conformational volume of -6.5 ± 0.2 ml/mol and -6.7 ± 0.3 ml/mol at 305 K and 310 K, respectively. These values are small compared with the size of the protein, and according to recent semiempirical calculations (Kharakoz, 1992) they are consistent with the formation of three hydrogen bonds or the ionization of at most two residues during the transformation of $bR^{all\text{-}trans}$ to $bR^{13\text{-}cis}$. In these expressions, the minus sign implies that the 13-*cis* isomer has a smaller volume than the all-*trans* isomer. In terms of the Gibbs free energy landscapes, this means that the potential well for the 13-*cis* isomer becomes deeper with increasing pressure, and this isomer is favored over the all-*trans* isomer. These findings are consistent with absorption measurements, although the latter can not directly determine the amount of all-*trans* and 13-*cis* pigments (Tsuda and Ebrey, 1980; Kovacs et al., 1993).

Using chemical extraction techniques on pressurized samples, Tsuda and Ebrey (1980) found a conformational volume change between the two isomers to be -7.8 ± 3.2 ml/mol. Because it is impossible to extract the chromophores at high pressure, it is assumed that the protein does not significantly relax after a pressure jump performed at 273 K. Moreover, the yield of the extraction is not 100%, but typically 75%. From a practical point of view, this complex process is very time consuming. The advantage of our method is obvious: it is nondestructive, and near-infrared Raman spectroscopy allows the examination of the entire vibrational spectrum, providing an in situ probe of the chromophore structure at any desired pressure.

The temperature independence of the isomeric ratio at ambient pressure is consistent with the finding that both conformations have the same Gibbs free energy and thus the same population in thermal equilibrium. However, at high pressure the 13-*cis* isomer has a lower Gibbs free energy and $\Delta G_c \neq 0$. Because of the relation $\Delta G = \Delta H - T\Delta S$ the absence of a significant population change with temperature then implies that the enthalpy ΔH associated with the isomerization must be zero if there is no entropy difference ΔS between the two states.

Major differences between bR 13-*cis* and all-*trans* isomers are explained in the vibrational analysis of Mathies and co-workers (Smith et al., 1987a,b) by isomerizations about the $C_{13}{=}C_{14}$ and C=N bonds. The bR^{LA} to bR^{DA} transition then involves a concerted "bicycle pedal" isomerization (Smith et al., 1987b) as proposed by Orlandi and Schulten (1979). At high pressure the equilibrium is shifted toward the 13-*cis* isomer because of its smaller volume and the fact that thermal back-conversion requiring double isomerization is less favorable.

Light to dark-adaptation kinetics

Time-resolved Raman spectra of the bR^{LA} to bR^{DA} adaptation at high pressure are shown in Fig. 6. Again, the Raman spectra for bR^{LA} exhibits a single-peak structure at 1526 cm^{-1}, corresponding to the all-*trans* isomer. With increasing time and pressure, we observe that the peak corresponding to the 13-*cis* isomer increases in intensity relative to the peak corresponding to the all-*trans* isomer. Fig. 7, displays an expanded view of the ethylenic region for kinetic Raman spectra at pressures of 0.1 and 170 MPa. The temperature in both cases is 300 K. It is evident from the spectra in Fig. 7 that the rate of dark adaptation speeds up with increasing temperature and pressure. We rule out the possibility that there is a significant change in pH with pressure. We have

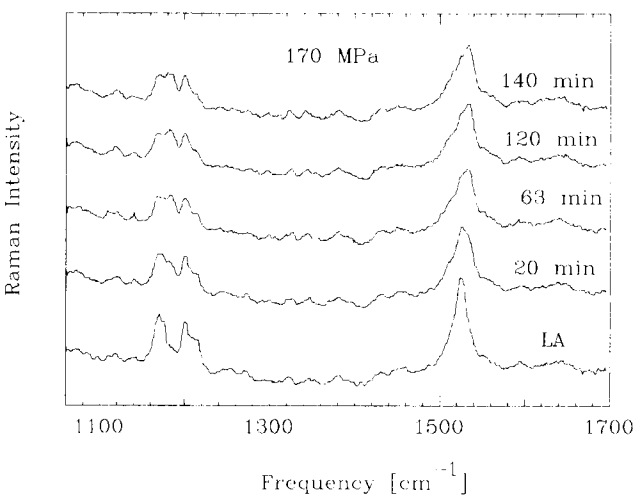

FIGURE 6 NIR Raman spectra of the light to dark adaptation kinetics at a pressure of 170 MPa (T = 300 K).

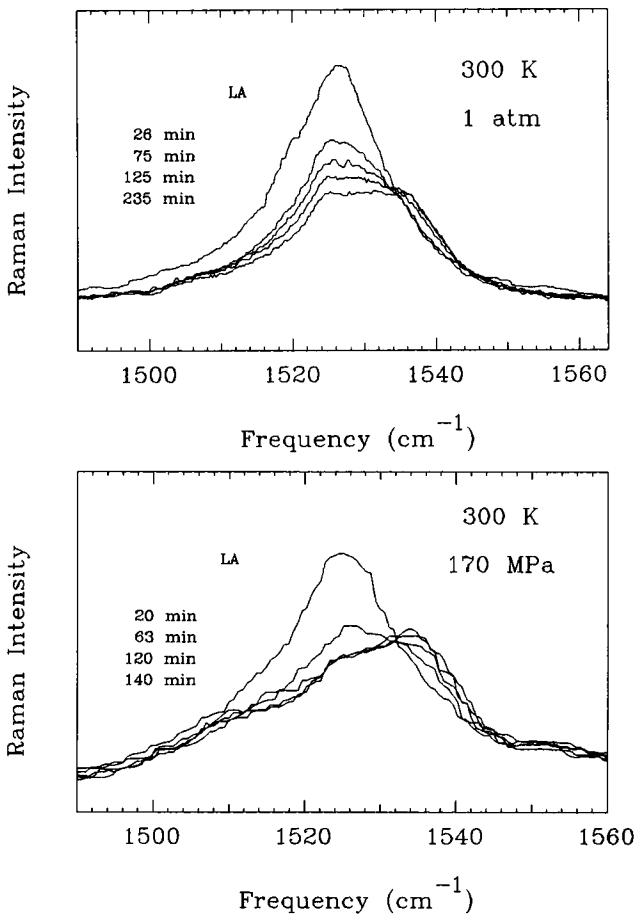

FIGURE 7 Expanded view of the ethylenic region of the NIR Raman spectra showing light to dark adaptation kinetics at 300 K. (*a*) Atmospheric pressure; (*b*) high pressure (170 MPa).

checked the absorption spectrum of our samples (bR^{LA}) at high pressure and observed a shift to longer wavelength by ≈4 nm immediately after raising the pressure to 170 MPa. This is consistent with the results of Tsuda and Ebrey (1980) and Kovacs et al. (1993) obtained in HCl or potassium phosphate buffers at pH 7. A decrease of pH with pressure would cause a significantly larger shift, for instance by 12 nm for a pH drop from 7 to below 5 (Dunach et al., 1990). On the other hand, there is little variation in the rate of dark adaptation with pH over the range from 6 to 8 (Ohno et al., 1977). We also observe only the all-*trans* isomer in the NIR Raman spectra of bR^{LA} at high pressure, whereas in low-pH blue membranes the presence of 13-*cis* isomers in bR^{LA} has been reported (Mowery et al., 1979).

To analyze the kinetics of the all-*trans* and 13-*cis* populations we define a relaxation function $\Phi(t)$ as

$$\Phi(t) = \frac{bR^{\text{all-}trans}(t) - bR^{\text{all-}trans}(\infty)}{bR^{\text{all-}trans}(0) - bR^{\text{all-}trans}(\infty)} = \frac{A_{\text{all-}trans}(t) - A_{\text{all-}trans}(\infty)}{A_{\text{all-}trans}(0) - A_{\text{all-}trans}(\infty)}. \quad (4)$$

Here, $\Phi(t)$ has been expressed in terms of the peak areas. The simplest scheme to describe a transition between $bR^{\text{all-}trans}$ and $bR^{13\text{-}cis}$ is a two-state model. In general, the rate coefficients can depend on temperature, pressure, and viscosity. Following Kovacs et al. (1993) we write

$$bR^{\text{all-}trans} \underset{k_{CT}}{\overset{k_{TC}}{\rightleftharpoons}} bR^{13\text{-}cis}. \quad (5)$$

Solving the rate equations, we arrive at the following equation:

$$[bR^{\text{all-}trans}(t) - bR^{\text{all-}trans}(\infty)] = [bR^{\text{all-}trans}(0) - bR^{\text{all-}trans}(\infty)]e^{-kt}, \quad (6)$$

where $k = k_{TC} + k_{CT}$, and

$$k_{CT} = k\frac{bR_{\text{all-}trans}(\infty)}{bR^{\text{all-}trans}(0)} = k_\kappa \quad (7)$$

$$k_{TC} = k[1 - \kappa]. \quad (8)$$

Here $\kappa = 1/(K_I + 1)$ represents the relative amount of all-*trans* isomers in $bR^{\text{all-}trans}$.

Fig. 8, shows the relaxation functions $\Phi(t)$ at 0.1 MPa and 170 MPa determined from the experimental data as well as fits with exponentials $\Phi(t) = \Phi_0 e^{-kt}$. The rate coefficients k obtained from these fits are summarized in Table 1. From the uncertainties in the determination of the areas and the least-squares fits to the kinetics we estimate a relative error of 25% for rate coefficients smaller than $4 \cdot 10^{-4}s^{-1}$. The errors become larger with faster rates, because the acquisition time for a spectrum is ≈100 s. The rate coefficients increase with both increased temperature and pressure. This result agrees with data derived from absorption measurements performed at high pressure by Kovacs et al. (1993) assuming the isomeric ratio is given. However, the Raman spectra directly monitor the isomeric composition during the light to dark adaptation, whereas the lack of structure in the broad absorption bands requires stringent assumptions to extract the rate constants.

The reaction rate coefficient can be written as

$$k(T, P) = \nu \exp\left[-\frac{G^\ddagger}{RT}\right] = A \exp\left[-\frac{H^\ddagger}{RT}\right], \quad (9)$$

where v, $H^\ddagger$, and $A = \nu \exp(S^\ddagger/R)$ are the frequency factor, activation enthalpy, and preexponential, respectively.

$$G^\ddagger = E^\ddagger + PV^\ddagger - TS^\ddagger \quad (10)$$

is the activation Gibbs free energy. $E^\ddagger$, $S^\ddagger$, and $V^\ddagger$ denote activation energy, entropy, and the activation volume of the reaction. Depending on the sign of $V^\ddagger$, the factor $e^{-PV^\ddagger/RT}$ pressure can either speed up or slow down the reaction rate.

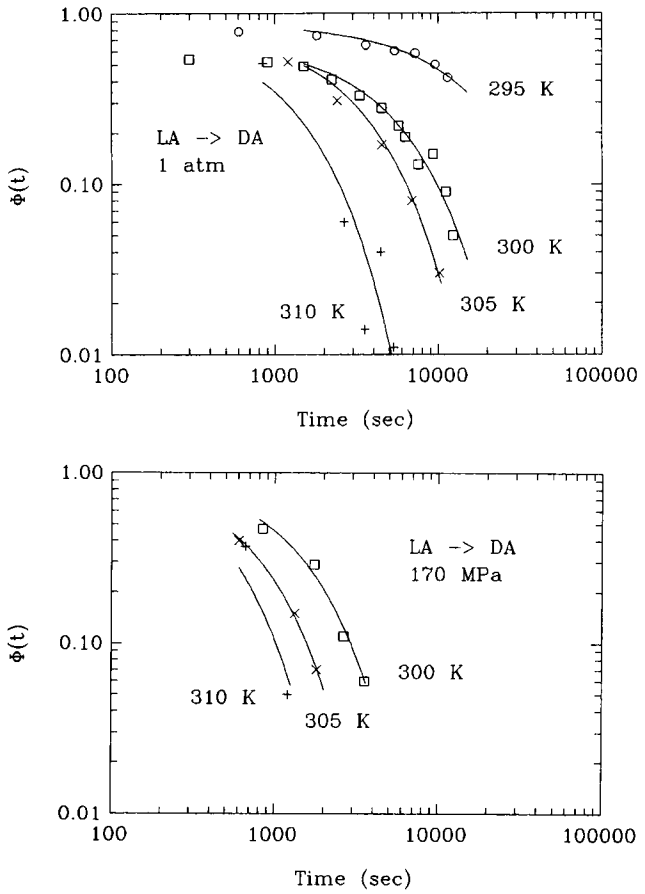

FIGURE 8 Relaxation functions $\Phi(t)$ determined from the kinetic Raman spectra during dark adaptation (see text) at atmospheric pressure (*a*) and at 170 MPa (*b*). The temperatures are indicated.

Given the rate coefficients at two pressures, the activation volume is expressed as (Johnson et al., 1974; Jonas and Jonas, 1994)

$$V^{\ddagger} = -\frac{RT}{P - P_o} \ln\left[\frac{k_P}{k_{P_o}}\right] \tag{11}$$

where k_p and k_{p0} are the rate constants at temperature T and pressures P and P_o, respectively.

For a reacting system consisting of two components there are two ways to go over the barrier. In general, the activation free energies will not be equal, so the activation volumes will be different. For bacteriorhodopsin, we denote $V^{\ddagger}_{TC}$ as the activation volume to go from the all-*trans* to 13-*cis* isomer, and $V^{\ddagger}_{CT}$ for the reverse process. From Eq. 11 and the rates measured at 0.1 and 170 MPa for temperatures of 300, 305, and 310 K we find average values $V^{\ddagger}_{TC} = -22$ ml/mol and $V_{CT} = -16.3$ ml/mol, respectively, with a standard deviation of 3.5 ml/mol. The minus sign indicates that the transition state has a smaller partial volume than either $bR^{13\text{-}cis}$ or $bR^{all\text{-}trans}$. These findings agree with the result that pressure favors the 13-*cis* isomer; it takes less energy for a *trans* to *cis* conversion than a *cis* to *trans* conversion. In addition to geometrical factors such as modifications in bond lengths and bond angles there are other important contributions to the activation volume. These include solvation, creation of hydrogen bonds and ionization changes. In recent calculations the volume effect of formation of one hydrogen bond in solution was found to be −2.2 mol/mol (Kharakoz, 1992). Volume changes accompanying ionization changes of weak acids are in the range of −10 to 20 ml/mol (Neuman et al., 1973). The difference in activation volumes ($V^{\ddagger}_{TC} - V^{\ddagger}_{CT}$) is −5.7 ml/mol and corresponds to the volume difference between $bR^{13\text{-}cis}$ and $bR^{all\text{-}trans}$. As a comparison, the conformational or reaction volume from the equilibrium isomeric ratio is about −6.6 ml/mol. Although there may be some limitations in the application of transition state theory the agreement between the results from the kinetics and the independent measurement of the equilibrium constant indicates the consistency of the activation volumes.

The large activation volume and the increase of the rate of thermal isomerization with pressure are interesting because of the possibility of progression through an intermediate state involving a protonation change. Balashov et al. (1993) have recently investigated the dark adaptation of a bR mutant, where Arg82 is replaced by an alanine. They suggest that the catalytic effect of an intermediate state requires that Asp85 be transiently protonated. Protonation of Asp85 will decrease the negative charge near the Schiff base nitrogen, which will cause an increase of the delocalization of π-electrons in the chromophore and result in a smaller barrier for isomerization (Warshel and Ottolenghi, 1979). The coupling of charge stabilization, torsion, and bond alternation is explained by calculations of Warshel and Deakyne (1978). It is conceivable that pressure decreases the negative charge near the Schiff base by changing the protonation state of a group close to the retinal. In as much as neutron diffraction (Papadopoulos et al., 1990) and recent FTIR studies (Maeda et al., 1994; Fischer et al., 1994) have detected several water molecules buried in the interior region of bR, a rearrangement of water molecules and hydrogen bonds due to pressure should alter the charge distribution as well. Results of molecular dynamics simulations indicate indeed that water affects the nature of the Schiff base counter-ion and the nature of the primary photoreaction (Zhou et al., 1993).

Fig. 9 shows Arrhenius plots of the rate coefficients, k_{TC} and k_{CT}, as a function of temperature. The results of least-squares fits to an Arrhenius expression (Eq. 9) for the activation enthalpy, $H^{\ddagger}$, and preexponential, A, are summarized in Table 2. The activation enthalpies are considerably larger than the thermal energy RT (=2.5 kJ/mol at 295 K). As a comparison, these values are also much higher than the activation enthalpies involved in the ligand-binding process for myoglobin (Frauenfelder et al., 1990). In addition, we observe that the preexponential, A, decreases with pressure, which is possibly due to a large change in the activation entropy. This is at variance with the conclusion by Kovacs et al. (1993) that the preexponential increases with pressure.

TABLE 1 Rate coefficients for light to dark-adaptation kinetics at atmospheric and high pressure

	0.1 MPa			170 MPa		
T(K)	$k(10^{-4}s^{-1})$	$k_{TC}(10^{-4}s^{-1})$	$k_{CT}(10^{-4}s^{-1})$	$k(10^{-4}s^{-1})$	$k_{TC}(10^{-4}s^{-1})$	$k_{CT}(10^{-4}s^{-1})$
295	0.6	0.3	0.3			
300	2	1	1	8	4.8	3.2
305	3.2	1.6	1.6	14	8.4	5.6
310	9	4.5	4.5	25	15	10

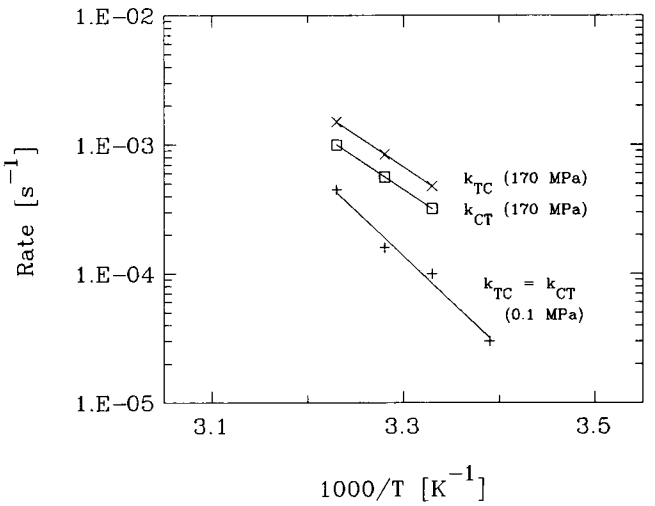

FIGURE 9 Arrhenius plot of the rate coefficients k_{TC} and k_{CT} of $bR^{all\text{-}trans} \rightleftharpoons bR^{13\text{-}cis}$ conversion at 0.1 and 170 MPa.

TABLE 2 Activation enthalpies, $H^{\ddagger}$, and preexponentials, A from Arrhenius fit to rate coefficients

	$H^{\ddagger}$/(kJ/mol)		log (A/s^{-1})	
P/MPa	k_{TC}	k_{CT}	k_{TC}	k_{CT}
0.1	131	131	19	19
170	95	95	13.2	13

A possible source of this contradiction may lie in the different techniques or pressures (170 and 340 MPa) employed. The calculation of the rate coefficients k_{TC} and k_{CT} requires the isomeric ratio determined here from the NIR Raman spectra under the same conditions as the kinetics. On the other hand, Kovacs et al. (1993) use the results of Tsuda and Ebrey (1980), which are available only at lower pressure (250 MPa compared to 340 MPa).

The large change in the preexponential of the Arrhenius expression with pressure may indicate the limitations of transition state theory (Johnson et al., 1974), which provides a justification for Eq. 9. Transition state theory cannot account for frictional forces along the reaction coordinates and the dependence of the rate coefficient on viscosity (Frauenfelder and Wolynes, 1985). The coefficients determined from an Arrhenius plot will therefore contain contributions due to pressure and temperature dependence of viscosity in addition to the part from the protein. In studies of the bR photocycle the solvent viscosity has been accounted for by a modified Kramers equation (Beece et al., 1981). The increase of solvent viscosity with pressure will lead to a decrease of the preexponential. A slowing down of the photocycle kinetics with pressure has been attributed to the increase of the internal viscosity of the purple membrane (Marque and Eisenstein, 1984). The interpretation of viscosity effects on the photocycle kinetics in glycerol-water solutions has recently been called into question by Cao et al. (1991). Their findings indicate that water activity strongly influences the M-decay rates. On the other hand light to dark adaptation kinetics speeds up with pressure, which suggests a dominating effect via the activation volume. To address this issue further, studies of the solvent dependence of the light to dark conversion are needed. The lack of data may be explained by the overlap of the bR^{LA} and bR^{DA} absorption bands; however, NIR Raman spectroscopy should provide an efficient tool for such investigations.

CONCLUSIONS

The ethylenic mode as well as C-C single stretches in the fingerprint region show that high pressure favors the 13-*cis* over the all-*trans* isomer. Raman spectroscopic measurements of the light to dark adaptation kinetics provide rate constants at variable temperature and pressure. Based on direct spectroscopic evidence we show that the rate constants increase with higher temperature and pressure. The data can be explained with a simple two-state model (13-*cis* and all-*trans*), yielding conformational and activation volumes for the light to dark adaptation in bacteriorhodopsin.

We thank T. Ebrey and R. Govindjee for providing bacteriorhodopsin and for discussions. L. Bradley II would like to thank the Mercury 7 Foundation for a scholarship. Support from the University of Central Florida through start-up funds and from the National Science Foundation (MCB-9305711) is gratefully acknowledged.

REFERENCES

Aton, B., A. G. Doukas, R. H. Callender, and T. G. Ebrey. 1979. Resonance Raman study of the dark-adapted form of the purple membrane protein. *Biochim. Biophys. Acta.* 576:424–428.

Balashov, S. P., R. Govindjee, M. Kono, E. Imasheva, E. Lukashev, T. G. Ebrey, R. K. Crouch, D. R. Menick, and Y. Feng. 1993. Effect of the arginine-82 to alanine mutation in bacteriorhodopsin on dark-adaptation, proton release, and the photochemical cycle. *Biochemistry.* 32: 10331–10343.

Beece, D., S. F. Bowne, J. Czege, L. Eisenstein, H. Frauenfelder, D. Good, M. C. Marden, J. Marque, P. Ormos, L. Reinisch, and K. T. Yue. 1981. The effect of viscosity on the photocycle of bacteriorhodopsin. *Photochem. Photobiol.* 33:517–522.

Birge, R. R. 1990. Nature of the primary photochemical event in rhodopsin and bacteriorhodopsin. *Biochim. Biophys. Acta.* 1016:293–327.

Cao, Y., G. Varo, M. Chang, B. Ni, R. Needleman, and J. K. Lanyi. 1991. Water is required for proton transfer from aspartate-96 to the bacteriorhodopsin Schiff base. *Biochemistry.* 30:10972–10979.

Dencher, N. A., K. D. Kohl, and M. P. Heyn. 1983. Photochemical cycle and light-dark adaptation of monomeric and aggregated bacteriorhodopsin in various lipid environments. *Biochemistry.* 22:1323–1334.

Dunach, M., S. Berkowitz, T. Marti, Y. W. He, S. Subramaniam, H. G. Khorana, and K. J. Rothschild. 1990. Ultraviolet-visible transient spectroscopy of bacteriorhodopsin mutants. *J. Biol. Chem.* 265: 16978–16984.

Fischer, W. B., S. Sonar, T. Marti, H. G. Khorana, and K. J. Rothschild. 1994. Detection of a water molecule in the active-site of bacteriorhodopsin: hydrogen bonding changes during the primary photoreaction. *Biochemistry.* 33:12757–12762.

Frauenfelder, H., N. Alberding, A. Ansari, D. Braunstein, B. R. Cowen, M. K. Hong, I. E. T. Iben, J. B. Johnson, S. Luck, J. R. Mourant, P. Ormos, L. Reinisch, R. Scholl, A. Schulte, E. Shyamsunder, L. B. Sorensen, P. J. Steinbach, A. H. Xie, R. D. Young, and K. T. Yue. 1990. Proteins and pressure. *J. Phys. Chem.* 94:1024–1037.

Frauenfelder, H., and P. G. Wolynes. 1985. Rate theories and puzzles of heme protein kinetics. *Science.* 229:337–345.

Henderson, R., J. M. Baldwin, T. A. Ceska, F. Zemlin, E. Beckmann, and K. H. Downing. 1990. Model for the structure of bacteriorhodopsin based on high-resolution electron cryomicroscopy. *J. Mol. Biol.* 213: 899–929.

Johnson, C. K., and R. Rubinovitz. 1991. Near-infrared excitation of Raman scattering by chromophoric proteins. *Spectrochim. Acta.* 47A: 1413–1421.

Johnson, F., H. Eyring, and B. Stover. 1974. The Theory of Rate Processes in Biology and Medicine. Wiley, New York.

Jonas, J., and A. Jonas. 1994. High-pressure NMR spectroscopy of proteins and membranes. *Annu. Rev. Biophys. Biomol. Struct.* 23:287–318.

Kharakoz, D. P. 1992. Partial molar volumes of molecules of arbitrary shape and the effect of hydrogen bonding with water. *J. Solution Chem.* 21:569–595.

Kovacs, I., G. U. Nienhaus, R. Philipp, and A. Xie. 1993. Pressure effects on the dark-adaptation of bacteriorhodopsin. *Biophys. J.* 64:1187–1193.

Lanyi, J. K. 1992. Bacteriorhodopsin: a light-driven proton pump in *Halobacterium halobium. Biophys. J.* 15:955–962.

Long, D. A. 1977. Raman Spectroscopy. McGraw-Hill, New York.

Maeda, A., J. Sasaki, Y. Yamazaki, R. Needleman, and J. K. Lanyi. 1994. Interaction of aspartate-85 with a water molecule and the protonated Schiff base in the L-intermediate of bacteriorhodopsin: a Fourier-transform infrared study. *Biochemistry.* 33:1713–1717.

Marque, J., and L. Eisenstein. 1984. Pressure effects on the photocycle of purple membrane. *Biochemistry.* 23:5556–5563.

Mathies, R. A., S. W. Lin, J. B. Ames, and W. T. Pollard. 1991. From femtoseconds to biology: mechanism of bacteriorhodopsin's light-driven proton pump. *Annu. Rev. Biophys. Biophys. Chem.* 20:491–518.

Mathies, R. A., S. O. Smith, and I. Palings. 1987. Determination of retinal chromophore structure in rhodopsins. *In* Biological Applications of Raman Spectroscopy, Vol. 2. T. G. Spiro, editor. Wiley, New York. 59–108.

Mattioli, T. A., A. Hoffmann, D. G. Sockalingum, B. Schrader, B. Robert, and M. Lutz. 1993. Application of near-IR Fourier transform resonance Raman spectroscopy to the study of photosynthetic proteins. (and references therein) *Spectrochim. Acta.* 49A:785–799.

Mowery, P. C., R. H. Lozier, Q. Chae, Y. W. Tseng, M. Taylor, and W. Stoeckenius. 1979. Effect of acid pH on the absorption spectra and photoreactions of bacteriorhodopsin. *Biochemistry.* 18:4100–4107.

Neuman, R. C., W. Kauzmann, and A. Zipp. 1973. Pressure dependence of weak acid ionization in aqueous buffers. *J. Phys. Chem.* 22:2687–2691.

Oesterhelt, D., M. Meentzen, and L. Schuhmann. 1973. Reversible dissociation of the purple complex in bacteriorhodopsin and identification of 13-*cis* and all-*trans*-retinal as its chromophore. *Eur. J. Biochem.* 40: 453–463.

Oesterhelt, D., and W. Stoeckenius. 1971. Rhodopsin like proteins from the purple membrane of *Halobacterium halobium. Nature New Biol.* 233: 149–152.

Ohno, K., Y. Takeuchi, and M. Yoshida. 1977. Effect of light-adaptation on the photoreaction of bacteriorhodopsin from halobacterium halobium. *Biochim. Biophys. Acta.* 462:575–582.

Orlandi, G., and K. Schulten. 1979. Coupling of stereochemistry and proton donor-acceptor properties of a Schiff base. A model of a light-driven proton pump. *Chem. Phys. Lett.* 64:370–374.

Papadopoulos, G., N. A. Dencher, G. Zaccai, and G. Bult. 1990. Water molecules and exchangeable hydrogen ions at the active centre of bacteriorhodopsin localized by neutron diffraction. *J. Mol. Biol.* 214: 15–19.

Pettei, M. J., A. P. Yudd, K. Nakanishi, R. Henselman, and W. Stoeckenius. 1977. Identification of retinal isomers isolated from bacteriorhodopsin. *Biochemistry.* 16:1955–1959.

Rath, P., M. P. Krebs, Y. He, H. G. Khorana, and K. J. Rothschild. 1993. Fourier transform Raman spectroscopy of the bacteriorhodopsin mutant Tyr-185→Phe: formation of a stable O-like species during light-adaptation and detection of its transient N-like photoproduct *Biochemistry.* 32:2272–2281.

Sawatzki, G., R. Fischer, H. Scheer, and F. Siebert. 1990. Fourier transform Raman spectroscopy applied to photobiological systems. *Proc. Natl. Acad. Sci. USA.* 87:5903–5906.

Scherrer, P., M. K. Mathew, W. Sperling, and W. Stoeckenius. 1989. Retinal isomer ratio in dark-adapted purple membrane and bacteriorhodopsin monomers. *Biochemistry.* 28:829–834.

Schulte, A. 1992. Near-infrared Raman spectroscopy using CCD detection and a semiconductor bandgap filter for Rayleigh line rejection. *Appl. Spectrosc.* 46:891–893.

Schulte, A., L. Bradley II, and C. Williams. 1995. Equilibrium composition of retinal isomers in dark-adapted bacteriorhodopsin and effect of high pressure probed by near-infrared Raman spectroscopy. *Appl. Spectrosc.* 49:80–83.

Smith, S. O., M. S. Braiman, A. B. Myers, J. A. Pardoen, J. M. L. Courtin, C. Winkel, J. Lugtenburg, and R. M. Mathies. 1987a. Vibrational analysis of the all-*trans*-retinal chromophore in light-adapted bacteriorhodopsin. *J. Am. Chem. Soc.* 109:3108–3125.

Smith, S. O., J. A. Pardoen, J. Lugtenburg, and R. A. Mathies. 1987b. Vibrational analysis of the 13-*cis*-retinal chromophore in dark-adapted bacteriorhodopsin. *J. Phys. Chem.* 91:804–819.

Stockburger, M., T. Alshuth, D. Oesterhelt, and W. Gärtner. 1986. Resonance Raman spectroscopy of bacteriorhodopsin: structure and function. *In* Spectroscopy of Biological Systems. R. J. H. Clark and R. E. Hester, editors. Wiley, New York. 483–535.

Stockburger, M., W. Klusmann, H. Gattermann, G. Massig, and R. Peters. 1979. Photochemical cycle of bacteriorhodopsin studied by resonance Raman spectroscopy. *Biochemistry.* 18:4886–4900.

Tsuda, M., and T. G. Ebrey. 1980. Effect of high pressure on the absorption spectrum and isomeric composition of bacteriorhodopsin. *Biophys. J.* 30:149–157.

Warshel, A., and C. Deakyne. 1978. Coupling of charge stabilization, torsion and bond alternation in light-induced reactions of visual pigments. *Chem. Phys. Lett.* 55:459–465.

Warshel, A., and M. Ottolenghi. 1979. Kinetic and spectroscopic effects of protein-chromophore electrostatic interaction in bacteriorhodopsin. *Photochem. Photobiol.* 30:291–293.

Weber, G., and H. G. Drickamer. 1983. The effect of high pressure upon proteins and other biomolecules. *Q. Rev. Biophys.* 16:89–112.

Zhou, F., A. Windemuth, and K. Schulten. 1993. Molecular dynamics study of the proton pump cycle of bacteriorhodopsin. *Biochemistry.* 32:2291–2306.